

**ARTICLE****Characteristics of Diesel/N-Butanol Blend on a Common Rail Diesel Engine with Exhaust Gas Recirculation**Yanfei Chen¹, Jingjing He^{2,*}, Hao Chen^{2,*}, Xin Su² and Bin Xie²¹Nanjing Vocational Institute of Transport Technology, Nanjing, 211188, China²School of Automobile, Chang'an University, Xi'an, 710064, China

*Corresponding Authors: Jingjing He. Email: hejj0117@126.com; Hao Chen. Email: colen7680@126.com

Received: 11 June 2021 Accepted: 29 December 2021

ABSTRACT

20% n-butanol is blended in diesel by volume (noted as D80B20) and experiment has been carried out to study the effect on the combustion and emission characteristics based on a common rail diesel engine with exhaust gas recirculation (EGR) system. The results reveal that D80B20 has longer ignition delay, shorter combustion duration and higher maximum in-cylinder temperature than pure diesel (noted as D100). Further, the number concentration and volume concentration of ultrafine particles decrease significantly while NO_x emissions increase a little with the addition of n-butanol. When the exhaust gas is induced into cylinder, NO_x emissions significantly decrease and ultrafine particles emissions increase. The number geometric mean diameters and volume geometric mean diameters of ultrafine particles increase with EGR ratio. Compared to D100 without EGR, D80B20 with 20% EGR ratio can reduce both NO_x and ultrafine particles emissions at 0.14 MPa BMEP and 0.56 MPa BMEP.

KEYWORDS

n-butanol; ultrafine particles; combustion; emission; common rail diesel engine

Abbreviations

ACMP	Accumulation mode particles
AKMP	Aitken mode particles
BMEP	Brake mean effective pressure
CA	Crank angle
CD	Combustion duration
D100	Pure diesel
D80B20	80% diesel and 20% n-butanol by vol.
EGR	Exhaust gas recirculation
EOC	End of combustion
ID	Ignition delay
LHV	Lower heating value
MHRR	Maximum heat release rate
MT	Maximum temperature



NC	Number concentration
NCMP	Nucleation mode particles
NGMD	Number geometric mean diameter
PM	Particulate matter
SOC	Start of combustion
SOI	Start of injection
UFPs	Ultrafine particles
VC	Volume concentration
VGMD	Volume geometric mean diameter

1 Introduction

Diesel engines emit high NO_x and particulate matters (PM) which are harmful for environment and human survival, especially the ultrafine particles (UFPs) emissions [1,2]. The mass concentration of UFPs can be negligible, while the number concentration is very high. UFPs can directly enter human respiratory system and cardiovascular system, which can lead to lung function changes, airway inflammation, anaphylaxis, thrombosis, endothelial function changes, atherosclerotic deterioration and so on [3–5]. In order to reduce the pollutant emissions of diesel engines, clean and alternative fuels for diesel have attracted substantial researches in recent years. Alcohols are common alternatives to reduce soot or PM emissions for oxygen content and low viscosity [6]. Chain alcohols can be divided into low carbon chain alcohols and high carbon chain alcohols according to the number of carbon atoms in molecular structure [7]. Higher oxygen content of low carbon chain alcohols helps reduce the PM emissions of diesel engines. As we all know that the oxygen content of methanol and ethanol reaches to 50% and 34.8%, respectively [8,9]. However, low carbon chain alcohols have strong polarity and they can only form diesel/alcohol micro-emulsion blends fuel with cosolvents or surfactants, leading to the poor stability and poor application convenience [10]. In generally, low carbon chain alcohols are used in diesel engine through dual fuel system. The dual fuel engine system may increase the manufacturing cost due to the additional fuel supply system and injection system. In addition, low carbon chain alcohols have low cetane number indicating the poor ignitability. With the increasing of the number of carbon atoms in the molecular structure, the cetane number and lower heating value (LHV) of alcohol fuels increase [11–13]. Therefore, high carbon chain alcohols have better ignitability than low carbon chain alcohols. Furthermore, high carbon chain alcohols can completely be miscible with diesel. However, the oxygen content of alcohol fuels decreases with the length of the carbon chain, which is not conducive to the fuel full combustion and soot reduction.

Researches have confirmed n-butanol with molecular structure $\text{CH}_3(\text{CH}_2)_3\text{OH}$ is a promising diesel alternative. Previous studies on spray characteristics showed that adding n-butanol in diesel making the spray cone angle increase in most cases [14–17]. Wang et al. [18] found that the ignition delay (ID) prolonged and the premixed combustion ratio obviously increased with n-butanol addition. And the butanol addition can greatly reduce soot emission especially under high load, whereas it has worse effect on the NO_x emission under all engine loads. Zhou et al. [19] investigated the effect of n-butanol proportion in blends on engine combustion and emissions under a 4-cylinder diesel engine. They observed that the introduction of n-butanol achieved the goal of ultra-low soot emissions while it led to increased NO_x emissions. Chen et al. [20] observed that n-butanol/diesel blends increased combustion pressure slightly and accelerated combustion speed. Further, the effect of n-butanol/diesel blends on soot reduction improved with the blending ratio of n-butanol under all conditions. Siwale et al. [21] indicated that 5%, 10%, and 20% volume fraction of n-butanol in diesel can reduce the soot emissions by 55.5%, 77.8% and 85.1%, while increase the NO_x emissions by 10.3%, 32.3% and 54.4%,

respectively. Nabi et al. [22] examined the diesel/n-butanol blends by using a 6-cylinder diesel engine in accordance with the 13-Mode European Stationary Cycle. It was obviously evident that Bu6 (30% diesel and 70% n-butanol in volume) showed the lower indicated power and mean effective pressure than diesel. Zhang et al. [23] blended two different volume fractions (20% and 40%) of n-butanol into diesel fuel and they found that there had little effects on NO_x emission, but NO proportion decreased and NO_2 proportion increased with higher n-butanol fraction. Atmanlı et al. [24] found that the average brake torque, brake power, brake thermal efficiency (BTE) and exhaust gas temperature decreased, while brake specific fuel consumption (BSFC) increased with increasing presence of n-butanol from 30% to 60% in diesel/cotton oil/n-butanol blends. An experimental investigation was carried out on a variable compression ratio CI engine with n-butanol/diesel blends (10%–25% by volume) and the best results of performance and emissions were observed for 20% n-butanol-diesel blend (B20) at a higher compression ratio as compared to diesel while keeping the other parameters unchanged [25]. Zhou et al. [19] studied the blend fuel of 10%, 20%, and 30% n-butanol by volume in diesel. Results showed that the addition of n-butanol (10%, 20%, and 30%) produced significant reduction in CO and soot emissions under certain post injection strategies. Within the range of 10% and 20% EGR, adding 20% n-butanol in diesel can achieve a balance between combustion performance and emissions under certain post injection strategies.

On the whole, adding n-butanol in diesel obviously improved the spray atomization quality, increased the ID, decreased the combustion duration (CD), promoted the combustion quality and thereby increased the maximum temperature (MT) in the most engine loads. N-butanol/diesel blends could significantly reduce the soot and PM emissions while it resulted in higher NO_x emissions compared with pure diesel. Exhaust Gas Recirculation (EGR) system was introduced to some related experiments to decrease NO_x emission. By introducing exhaust gas into the cylinder, the MT in cylinder decreased and thereby the NO_x formation of diesel engine reduced. Experimental results showed that the NO_x emissions of n-butanol with 0% EGR rate decreased 50% and 58%, respectively, compared with 14% and 30% EGR rate [18,19]. He et al. [26] also found that with the introduction of 20% EGR ratio in D60G40 (40% gasoline and 60% diesel in volume) combustion, NO_x emissions decreased by 20% compared to the model without EGR.

Based on the summary of literature study, D80B20 (80% diesel and 20% n-butanol by volume) is chosen as the testing fuels in this study since it represents a good balance of combustion performance and emissions. And the increase of D80B20 in NO_x emission is balanced through EGR system. Further, there are seldom studies focused on both UFPs and NO_x emissions of diesel/n-butanol blends. Therefore, the effect of D80B20 on UFPs and NO_x emissions are comprehensively studied on a common rail diesel engine with EGR system in this work. In addition, the emission characteristics of UFPs after adding n-butanol to diesel have been systematically studied, including number concentration, volume concentration and diameter distribution, etc., which is helpful to fill in the gap in the research of n-butanol as diesel alternative.

2 Methodology

2.1 Fuels Properties

Test fuels are D100 (pure diesel) and D80B20. The main properties of D100 and D80B20 are tested and displayed in Table 1. The cetane number, lower heating value, kinematic viscosity and density of test fuels are measured in accordance with the standards of ASTM D 613, ASTM D 240, ASTM D 445 and ASTM D 1298. The cetane number is measured and obtained through the method of calibration and interpolation. The lower heating value is measured using an oxygen bomb calorimeter. The

kinematic viscosity is measured using a thermostatic capillary. The density is measured with a density meter (according to the principle of Archimedes). The uncertainties from measurement methods and processes could be neglected because the instruments, the measurement standard were fixed and the experimenters are also the same group. Further, the average of 5 repeated experiments is used as the final result, which can minimize the uncertainties. N-butanol has the low viscosity and distillation temperature, which improve the fluidity and volatility. Blending n-butanol is helpful to improve the spray atomization quality. However, the cetane number of n-butanol is only 16, resulting in a poor ignitability of D80B20. The LHV of D80B20 is 40.6 MJ/kg which is lower than 42.5 MJ/kg of D100.

Table 1: The properties of test fuels

Properties	D100	N-butanol	D80B20
Density (kg/m ³)	837	806	817
Cetane number	50	16	40
Viscosity at 20°C (mm ² /s)	4.37	2.51	3.82
Oxygen content (%)	0	21.6	4.38
Lower heating value (MJ/kg)	42.5	33.1	40.6
95% distillation temperature (°C)	358	217	296

2.2 Experiment Setup and Testing Procedure

The combustion and emission performances of test fuels are studied on a common rail diesel engine with EGR system. Table 2 gives parameters and specifications of the test engine. Fig. 1 shows the arrangement for test system. Injection pressures and injection timings are controlled through the BOSCH injection system. An electric dynamo meter (CAMA CW160B) is used to control the engine working torque and speed. The peak torque is achieved between 1600 and 1800 r/min. In this research, 1800 r/min is chosen. The torques of 50, 150, 200, 250, 300 and 350 Nm are chosen to represent different engine loads and the corresponding brake mean effective pressures (BMEP) are 0.14, 0.42, 0.56, 0.70, 0.84, and 0.98 MPa, respectively. The initial injection strategy includes pilot injection and main injection. A piezo-electric type pressure sensor (6052A, Kistler) used to measure the in-cylinder pressure is installed on the top of the first cylinder. And then the pressure signal is amplified and analyzed by a charge amplifier (5019B, Kistler) and a combustion analyzer (KIBOX, Kistler), respectively. A magnetoelectric crankshaft position sensor with the resolution of 0.1 degree crank angle (°CA) is applied to record the crank angle position. In each measurement, 100 consecutive cycles are recorded and averaged with the KiBox-Cockpit software. NO_x emissions are measured by MAHA MET6.X with volume concentrations and UFPs emissions are measured by an aerodynamic particle sizer spectrometer (TSI SMPS-3936). The range and accuracy of the test apparatus are shown in Table 3. The engine is warmed up under idling condition until the coolant temperature and the lubrication oil temperature satisfy with the requirement. When the test fuel is changed, the engine operates for 5 min to ensure previous fuel in fuel line and rail pipe have been consumed. In each condition, the engine operates stably for 3 min.

Table 2: Test engine parameters and specifications

Items	Parameters or specifications
Fuel injection system	Common rail
Engine type	in-line 4-cylinder, inter-cooled, turbocharged
Displacement (L)	4.5
Bore × stroke (mm)	105 × 130
Compression ratio	18

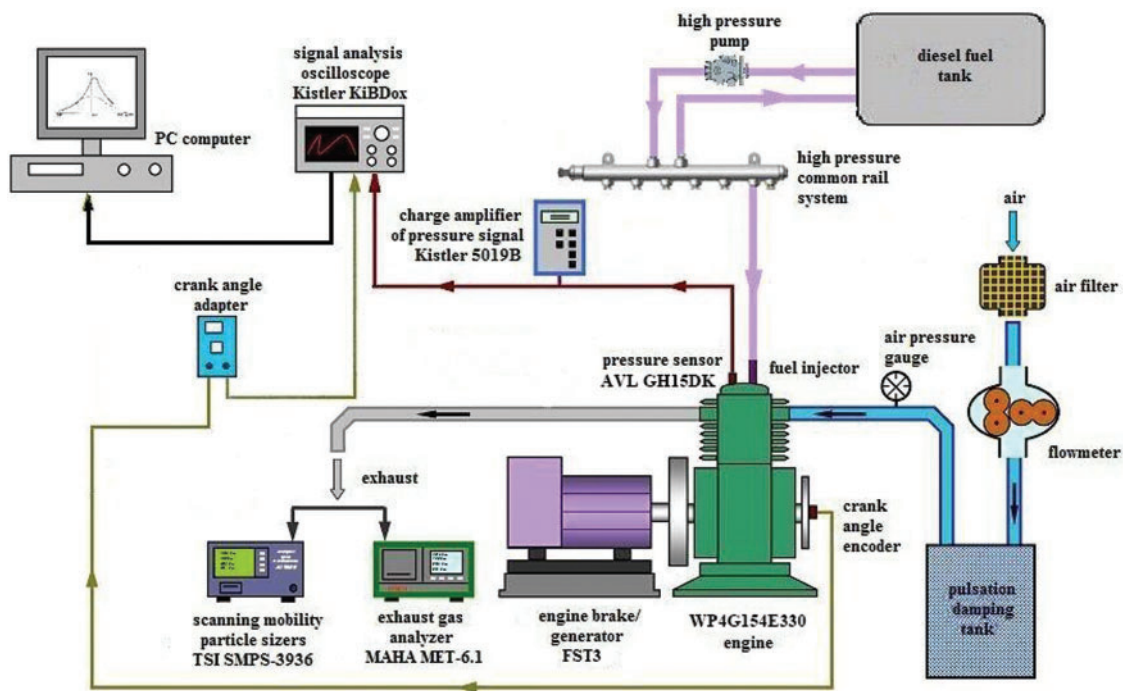


Figure 1: Engine system schematics

Table 3: The range and accuracy of the test apparatus

Apparatus	Measured parameters	Range	Accuracy
Electric dynamometer	Speed	0–10000 rpm	1%
	Torque	0–520 N·m	0.2%
Pressure sensor	in-cylinder pressure	0–25 MPa	0.1 MPa
MAHA MET6.X	NO _x	0–5000 ppm	±20 ppm
SMPS-3936	UFPs	2.5–1000 nm	10 nm

2.3 Data Processing

Based on the in-cylinder pressure, heat release rate and in-cylinder combustion temperature for diesel engines are calculated by a simplified apparent heat release model [27,28]. The heat release rate and temperature in cylinder can be calculated by Eqs. (1) and (2), number geometric mean diameter (NGMD) and volume geometric mean diameter (VGMD) are adopted for a typical diameter analysis of UFPs and the calculation are listed in Eqs. (3)–(7). The meaning represented by the letters in each equation is detailed in reference [10].

$$\frac{dQ}{d\phi} = \frac{k}{k-1} p \frac{dV}{d\phi} + \frac{1}{k-1} V \frac{dp}{d\phi} \quad (1)$$

$$\frac{dT}{d\phi} = \frac{1}{mc_v} \left(\frac{dQ}{d\phi} - p \frac{dV}{d\phi} \right) \quad (2)$$

$$NGMD = \exp \left[\frac{\sum_l^u n \times \ln D_p}{NC} \right] \quad (3)$$

$$VGMD = \exp \left[\frac{\sum_l^u v \times \ln D_p}{VC} \right] \quad (4)$$

$$NC = \sum_l^u n \quad (5)$$

$$VC = \sum_l^u v \quad (6)$$

$$n = \frac{c}{iQ} \times \frac{\phi}{\eta} \quad (7)$$

3 Combustion Characteristics

3.1 Effect of n-Butanol on Combustion Characteristics

In this study, the start of injection (SOI) is defined as the crank angle corresponding to the maximum driving current of the high pressure injector. The start of combustion (SOC) is defined as the zero point of heat release rate from the negative to positive and the end of combustion (EOC) is the zero point of heat release rate from the positive to negative. The ID is the period between SOI and SOC, and the CD is the period between SOC and EOC. Table 4 the specific parameters of test fuels. Table 5 lists the SOCs and EOCs of D100 and D80B20 under various engine loads. The IDs and CDs of test fuels are displayed in Fig. 2. The SOCs of D80B20 are always later than those of D100 for lower cetane number and worse ignitability. And thereby the IDs of D80B20 are longer than those of D100. Obviously, the ID decreases and the CD increases with engine load from Fig. 2. It can be also observed that the gap of IDs or CDs between D80B20 and D100 get smaller as engine load increases. The gap of SOC and EOC decreases as the load increases among fuels. This indicates that the reactivity differences do not play a significant role at high load cases since the ambient temperature and pressure are high enough at these high load cases. At 0.14 MPa BMEP low load, the ID of D80B20 is 10.5 °CA,

which is 1.08 °CA longer than D100. The temperature and pressure in cylinder increase as engine load increases. And at 0.98 MPa BMEP, the ID of D80B20 is 0.64 °CA longer than that of D100.

Table 4: The specific parameters of test fuels

BMEP	EGR rate	Inlet pressure (kPa)		Inlet temperature (°C)		Injection pressure (MPa)		Exhaust temperature (°C)		λ	
		D100	D80B20	D100	D80B20	D100	D80B20	D100	D80B20	D100	D80B20
0.14 MPa	0	102.9	103.6	43.5	51	57.8	58.8	161	180	5.11	5.09
	10%	103	103.5	43.6	51	57.7	58.7	164	180	5.21	5.01
	20%	102.9	103.4	43.8	50.9	57.5	58.7	165	178	4.93	4.89
	30%	102.9	103.5	43.7	50.8	57.4	58.7	166	177	3.06	4.72
	40%	103.1	103.3	45.4	50.8	57.4	58.7	168	174	4.75	4.62
0.42 MPa	0	115	113.3	46	50.8	75.2	73.6	213	220	2.94	3.02
0.56 MPa	0	122	121	48.7	51.5	80.7	82.4	273	255	2.46	2.59
	10%	123	122.9	48.9	52.2	80.6	82.4	277	273	2.55	2.50
	20%	122.8	124	49.2	52.8	80.4	82.6	280	285	2.51	2.43
	30%	122.8	123.6	49.3	53.1	80.2	82.8	280	288	2.44	2.37
	40%	123.2	124	49	53	79.9	82.4	280	289	2.40	2.32
0.70 MPa	0	133.8	131.5	48.8	52.8	89.3	89.9	298	300	2.27	2.27
0.84 MPa	0	141.6	139.5	49.5	53.7	97	97.4	325	333	2.08	2.1
0.98 MPa	0	151.7	152.3	50.6	54.9	101.8	103.6	356	360	1.96	1.9
	10%	152.3	153.2	51.8	55.7	101.7	103.6	364	374	1.9	1.86
	20%	153.2	154.3	52.7	56	101.6	103.8	369	377	1.85	1.8
	30%	154.4	155	52.4	55.5	101.5	103.5	373	377	1.81	1.76
	40%	155	155.6	52.3	55.4	102.1	103.3	372	380	1.76	1.71

Table 5: SOC and EOCs of D100 and D80B20

Engine loads	D100		D80B20	
	SOC (°CA)	EOC (°CA)	SOC (°CA)	EOC (°CA)
BMEP = 0.14 MPa	-9.6	21	-8.5	20
BMEP = 0.42 MPa	-11.6	30	-10.4	28
BMEP = 0.56 MPa	-12.5	33.2	-11.7	32.8
BMEP = 0.70 MPa	-13.6	39.2	-12.8	38.8
BMEP = 0.84 MPa	-14.4	43.3	-13.7	43.7
BMEP = 0.98 MPa	-14.8	47	-14.2	46

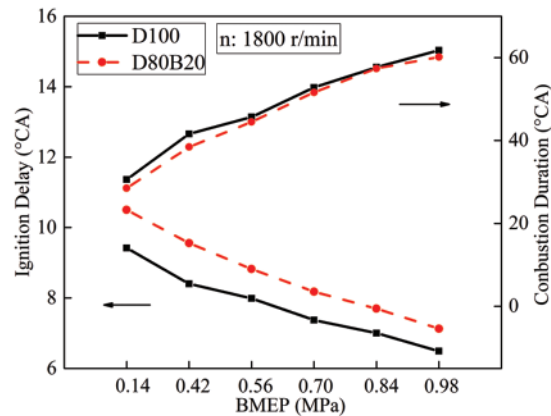


Figure 2: IDs and CDs of D100 and D80B20

Fig. 3 shows the pressure, temperature and heat release rate in cylinder of D100 and D80B20 at 0.14, 0.56, 0.98 MPa BMEP. Table 6 lists the maximum heat release rates (MHRRs) and MTs under different engine loads. It can be seen from Fig. 3a that the MHRR of D80B20 is significantly higher than D100 under low load. On the one hand, the pressure and temperature in cylinder are relatively low and the influence of low cetane number on ignition delay is obvious under low engine load. And long ID of D80B20 makes a large amount of the fuel/air mixture. On the other hand, the low viscosity and high volatility of D80B20 improves the spray quality and mixture uniformity. The spray particle size is mainly related to the viscosity and surface tension of the fuel. The lower the viscosity and surface tension, the easier the fuel spray breaks into smaller droplets [17]. Wu et al. [15] found that the air entrainment around the blend enhanced and the spray in front became more disorder after mixing n-butanol. In addition, the color of spray head was shallower than basic fuel, which suggested that spray particle size became smaller and the atomization was more uniform with n-butanol blending [15]. Accordingly, a large and uniform fuel/air mixture is beneficial to speed up the fuel combustion. Therefore, the premixed combustion strengthens and the MHRR increases with n-butanol addition. At 0.14 MPa BMEP, the MHRR of D80B20 is 37.09 J/°CA, increased by 2.4 J/°CA compared to diesel. Further, the MHRR gap between D80B20 and D100 gradually narrows with engine load. And when $BMEP \geq 0.84$ MPa, D80B20 has lower MHRRs than D100. As the load increases, the pressure and temperature in the cylinder increase gradually. In high in-cylinder thermal condition, the influence of fuel reactivity becomes less crucial and thereby the gap of ID between D100 and D80B20 becomes small. Meanwhile, the fraction of diffusion combustion becomes larger at high engine load cases. The high oxygen content of D80B20 can release a large number of oxygen atoms and active free radicals during the stage of diffusion combustion, which can speed up combustion speed and promote combustion completeness [26]. However, the LHV of the n-butanol is lower than that of diesel. As a result, under medium and high loads, the MHRR of D80B20 is lower than D100. Meanwhile, D80B20 has a higher heat release rate than D100 in the stage of diffusion combustion, which can be seen from Fig. 3c. It can also clearly be observed in Fig. 2 that the CD of D80B20 is always shorter than D100, which indicates the combustion heat release of D80B20 is more concentrated. Therefore, D80B20 has the high maximum temperatures under all conditions.

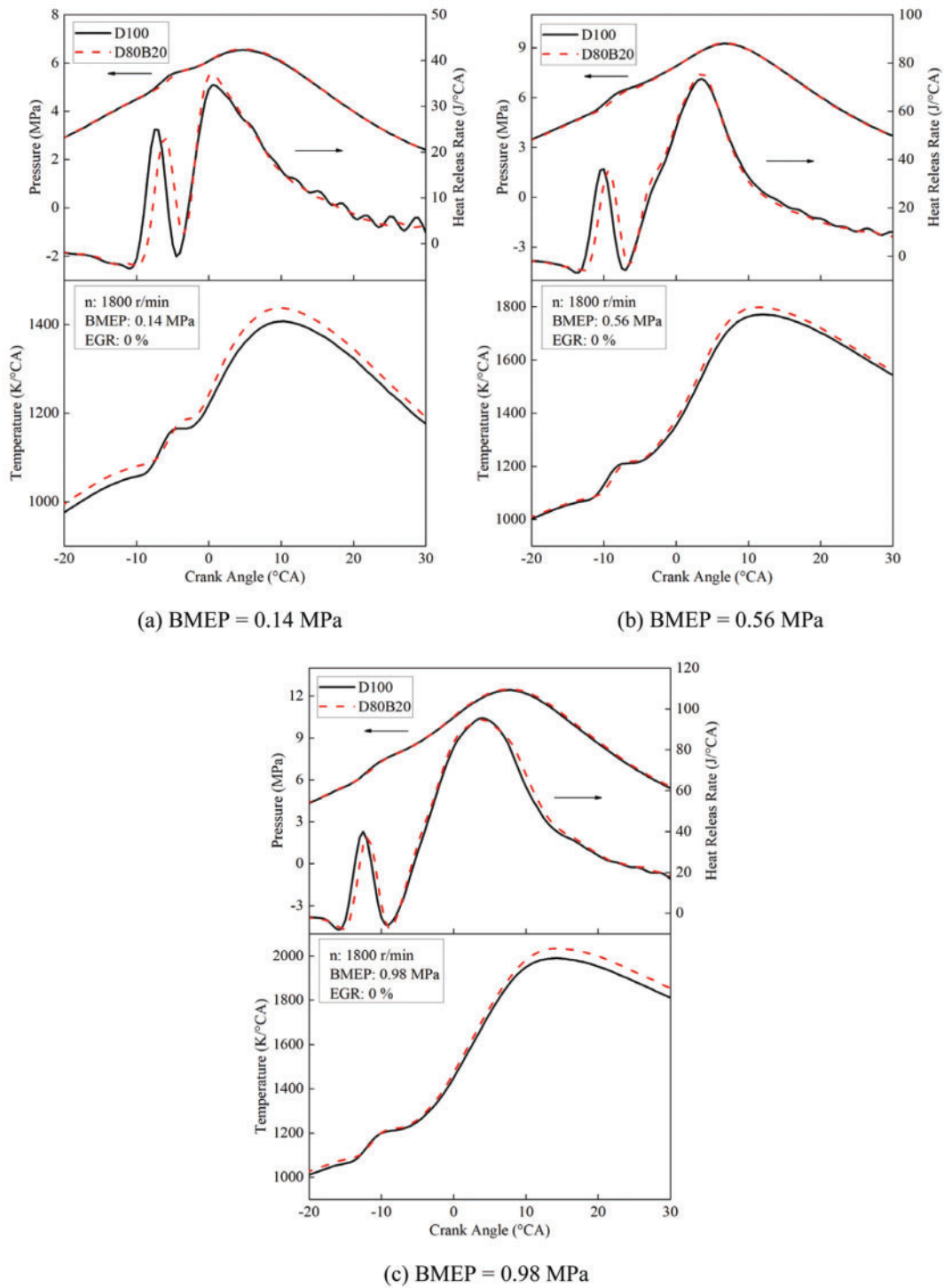


Figure 3: Pressure, heat release rate and temperature in cylinder

Table 6: MHRRs and MTs of test fuels at various loads

Engine loads	D100		D80B20	
	MHRR (J/°CA)	MT (K)	MHRR (J/°CA)	MT (K)
BMEP = 0.14 MPa	34.69	1407.3	37.09	1437.5
BMEP = 0.42 MPa	63.59	1682.2	61.90	1679.1
BMEP = 0.56 MPa	73.37	1771.5	75.69	1799.1
BMEP = 0.70 MPa	86.29	1865.9	86.90	1904.7
BMEP = 0.84 MPa	91.66	1946.3	90.24	1977.6
BMEP = 0.98 MPa	95.54	1989.0	94.81	2033.6

3.2 Effect of EGR Ratio on Combustion Characteristics

Table 7 displays the MHRRs and MTs of the test fuels with EGR at 0.56 and 0.98 MPa BMEP. With the increasing of EGR ratio, the MT decreases obviously.

Table 7: MHRRs and MTs of test fuels with various EGR ratio

EGR ratio (%)	BMEP = 0.56 MPa				BMEP = 0.98 MPa			
	D100		D80B20		D100		D80B20	
	MHRR (J/°CA)	MT (K)	MHRR (J/°CA)	MT (K)	MHRR (J/°CA)	MT (K)	MHRR (J/°CA)	MT (K)
0	73.37	1771.5	75.69	1799.1	95.54	1989.0	94.81	2033.6
10	73.58	1753.9	76.93	1817.3	95.77	1977.5	94.78	2018.4
20	72.48	1739.6	75.42	1789.5	95.15	1962.0	95.44	2012.2
30	71.78	1737.9	76.12	1795.2	95.10	1955.9	95.65	1987.9
40	70.25	1726.7	74.81	1780.1	93.68	1943.1	93.90	1990.1

4 Engine Emissions

4.1 NO_x Emissions

The NO_x emissions of D100 and D80B20 at 1800 r/min are shown in Fig. 4. It can be observed D80B20 has higher NO_x emissions than D100. Previous studies have shown that NO is the mainly composition of NO_x exhausted by diesel engine and meanwhile N₂ and O₂ can react and then produce NO easily when the temperature in cylinder is higher than 1500°C [29,30]. Accordingly, MT has a great influence on NO_x emissions [31]. The MTs of D80B20 are higher than those of D100 and thereby the NO_x emissions of D80B20 are higher than D100. Fig. 5 displays the influence of EGR ratio on NO_x emissions at 0.56 and 0.98 MPa. With the increasing of EGR ratio, the NO_x emissions of D100 and D80B20 both significantly decrease mostly due to the decreased MTs. As load increases, the reduction

degree of NO_x emissions with EGR ratio increases. The NO_x emission of D80B20 is always higher than that of D100, irrespective using EGR or not.

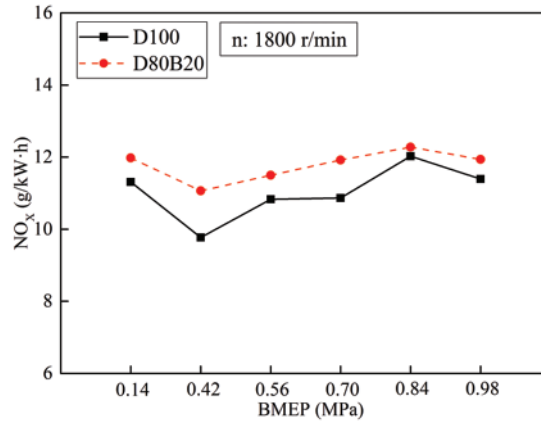


Figure 4: NO_x emissions of D100 and D80B20

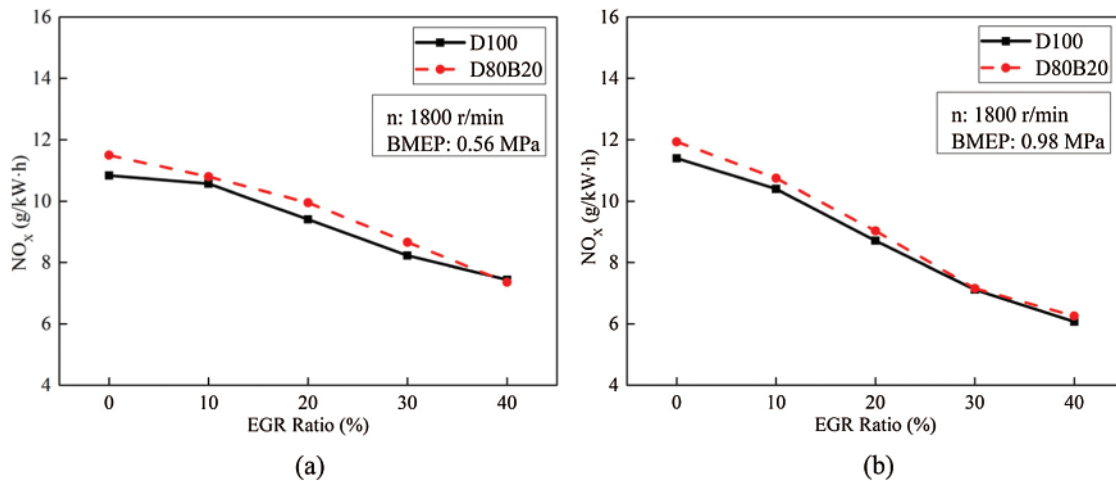


Figure 5: Effect of EGR ratio on NO_x emissions

4.2 UFPs Emissions

PM is one of the harmful exhaust pollutants emitted by diesel engines. 2.5~220 nm particles are defined as UFPs in this study. It has proved that more than 90% total PM number concentrations are UFPs. Nucleation mode particle (NCMP), aitken mode particle (AKMP) and accumulation mode particle (ACMP) are included in UFPs emitted by diesel engines. The diameter of NCMP is less than 50 nm, AKMP is between 50 and 100 nm and ACMP is between 100 and 220 nm [10]. The particles with a diameter in the range of 5~100 nm are mainly composed of volatile organic compounds and sulfates [32]. And the particles with a diameter greater than 100 nm are mainly composed of accumulated soot particles and substances attached to the surface [32]. There are differences in the deposition characteristics of particles with different diameters in the human body. Particles with small diameters, especially nuclear particles, are more likely to penetrate into the human respiratory system and endanger human health [3]. Fig. 6 shows the number concentrations (NCs) and volume

concentration (VCs) of UFPs under various loads. The diameter distributions of UFPs are displayed in Fig. 7. At 0.14 MPa BMEP, the low thermal condition is not conducive to fuel complete combustion and thereby the UFPs emissions are high. At 0.42 MPa BMEP, although the thermal condition in cylinder has improved, the amount of fuel injection increased. At this time, the quality of the fuel atomization in cylinder is worse than that of 0.14 MPa BMEP. Therefore, the UFPs emission at 0.42 MPa BMEP is higher than that of 0.14 MPa BMEP. The NCMPs and AKMPs of two fuels have a very large proportion in NCs while a very small proportion in VCs. The lower viscosity and distillation temperature of n-butanol making D80B20 has higher spray atomization quality and more uniform mixture than D100. In addition, the chemical mechanism of neat butanol is different from the n-butanol/alkane fuel blends. The oxidation of n-butanol starts with H abstraction in the alpha carbon due to the lowest BDE. And due to the reaction R2915, it forms stable butyraldehyde rather than QOOH radicals, degenerates the branching production of OH [33]. N-butanol additive can greatly reduce the UFPs emissions, and both the VCs and NCs reduced accordingly. At 0.70 MPa BMEP, the VCs and NCs of D80B20 decrease by 46.4% and 31.1% compared with D100.

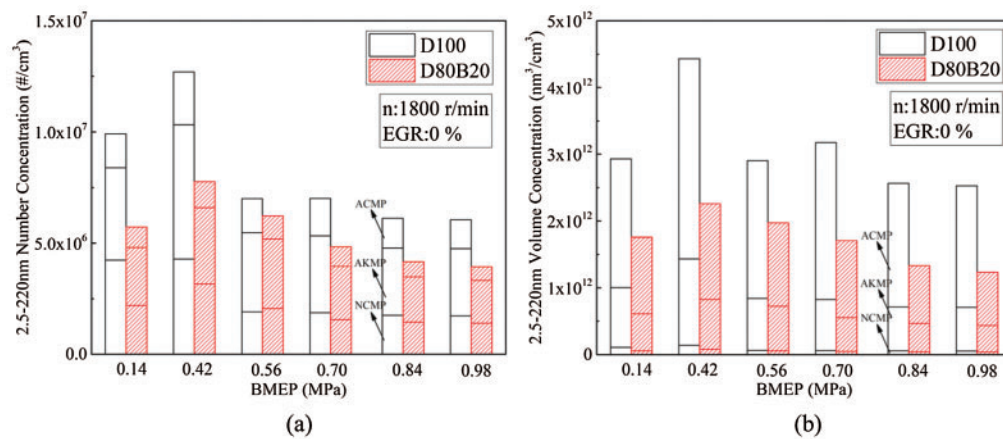


Figure 6: NCs and VCs of UFPs under various loads

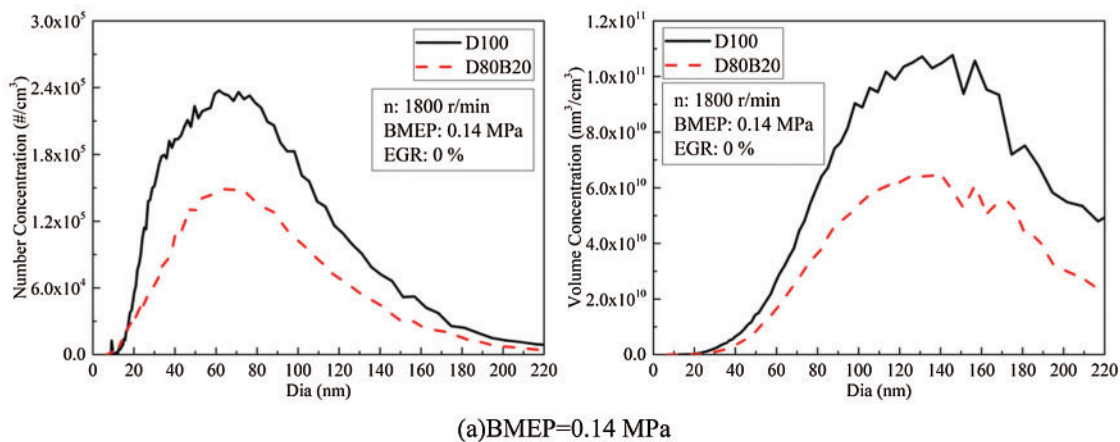


Figure 7: (Continued)

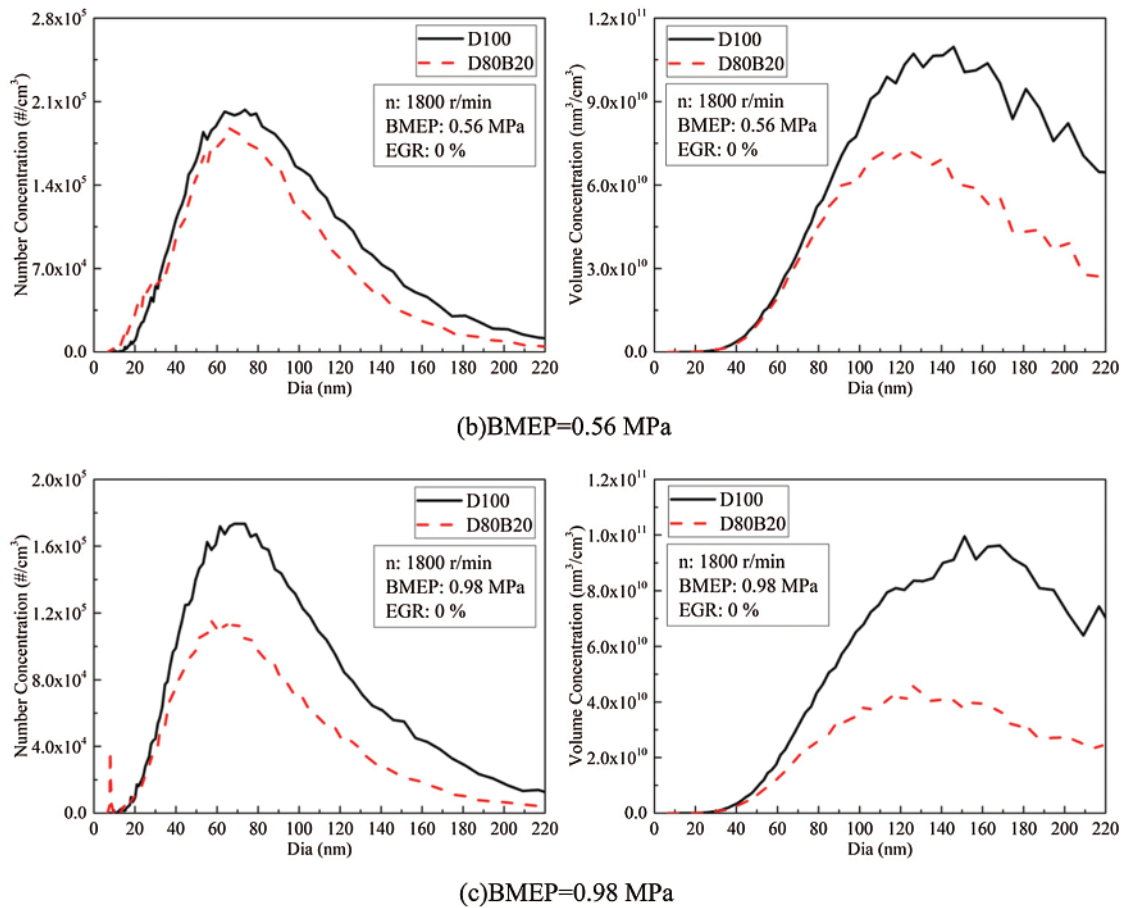


Figure 7: NCs and VCs diameter distributions of UFPs under various loads

Fig. 8 exhibits the effects of EGR ratios on NCs and VCs of UFPs at 0.14, 0.56 and 0.98 MPa BMEP. Fig. 9 displays the diameter distribution of UFPs under various EGR ratio. The NCs and VCs of UFPs increase with EGR ratio due to the worse combustion quality. At 0.14 MPa BMEP and 0.56 MPa BMEP, the NCs and VCs of D80B20 are at a low level when the EGR ratio is less than 30%. At 0.98 MPa BMEP, the UFPs emissions increase significantly with the increasing of EGR ratio. Further, D80B20 with 10% EGR ratio has a lower UFPs emissions than D100 without EGR. Table 8 gives the VGMDs and NGMDs of UFPs. The VGMDs and NGMDs of D80B20 are smaller than those of D100. Additionally, the NGMDs and VGMDs of increase with EGR ratio. For example, the NGMDs of D80B20 increases from 58.8 to 84.2 nm as EGR ratio increase from 0% to 40% at 0.98 MPa BMEP.

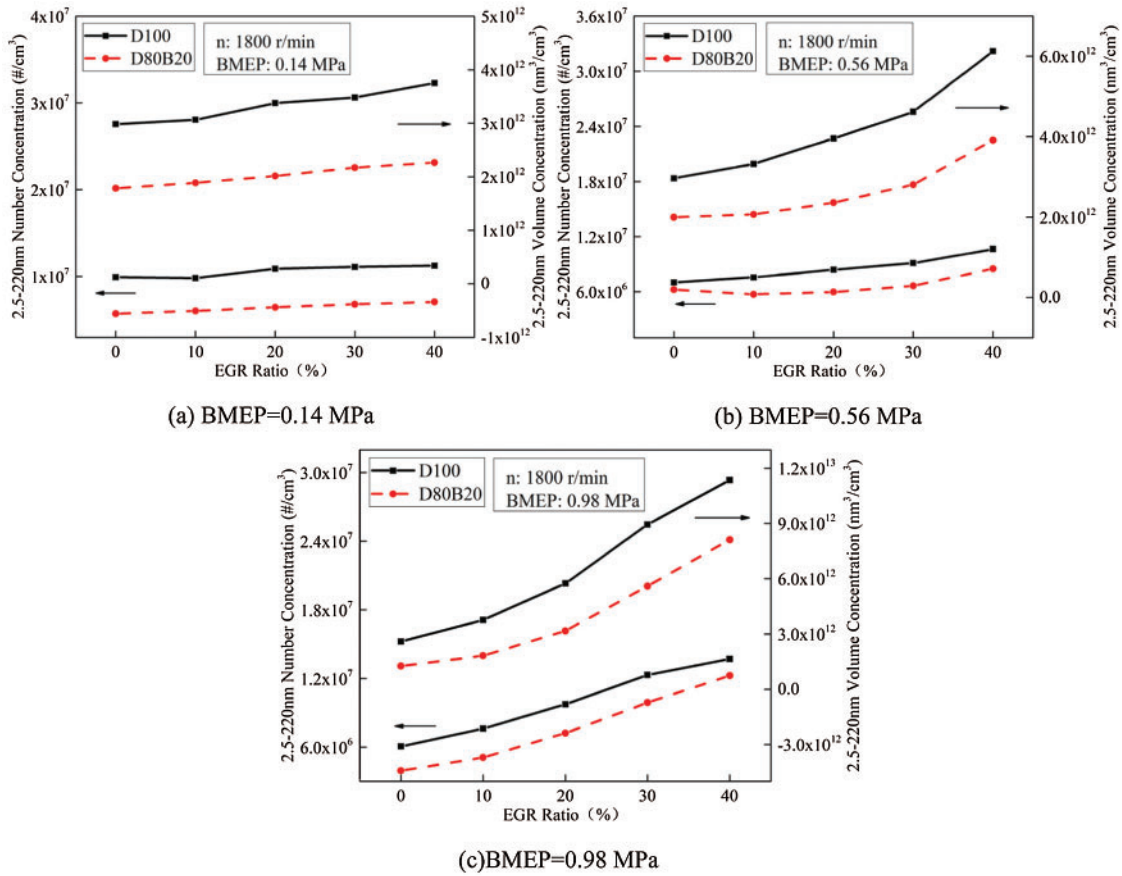
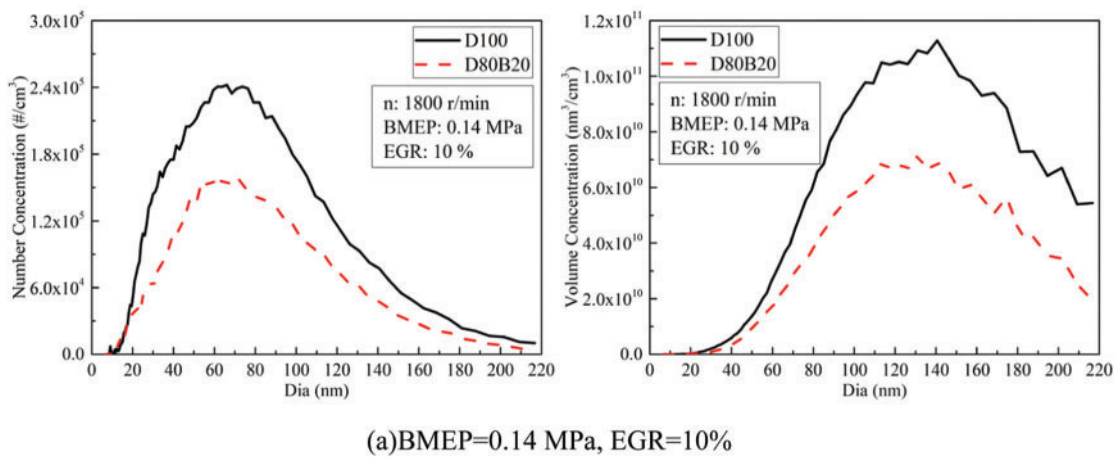
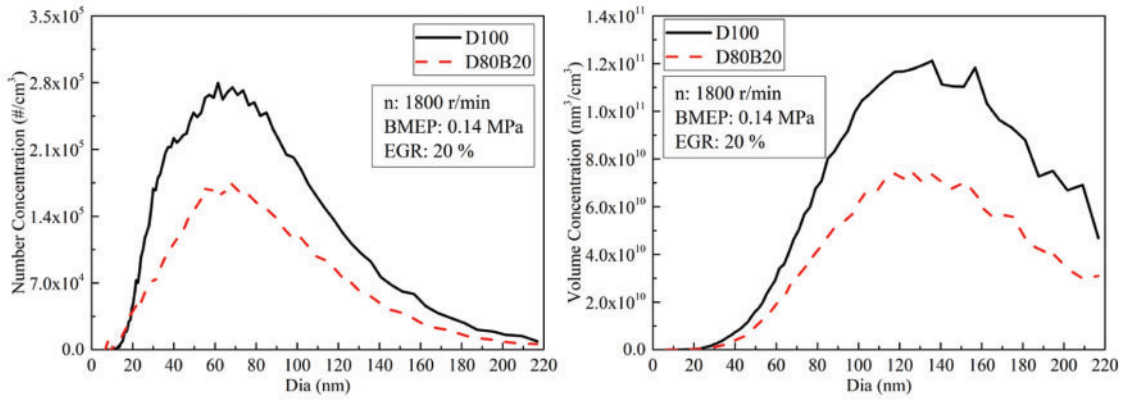


Figure 8: Effects of EGR ratio on NCs and VCs of UFPs

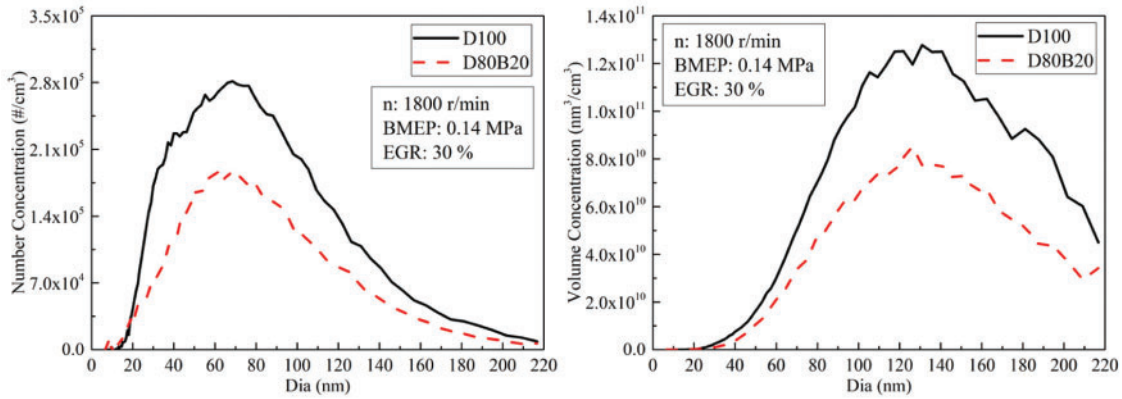


(a) BMEP=0.14 MPa, EGR=10%

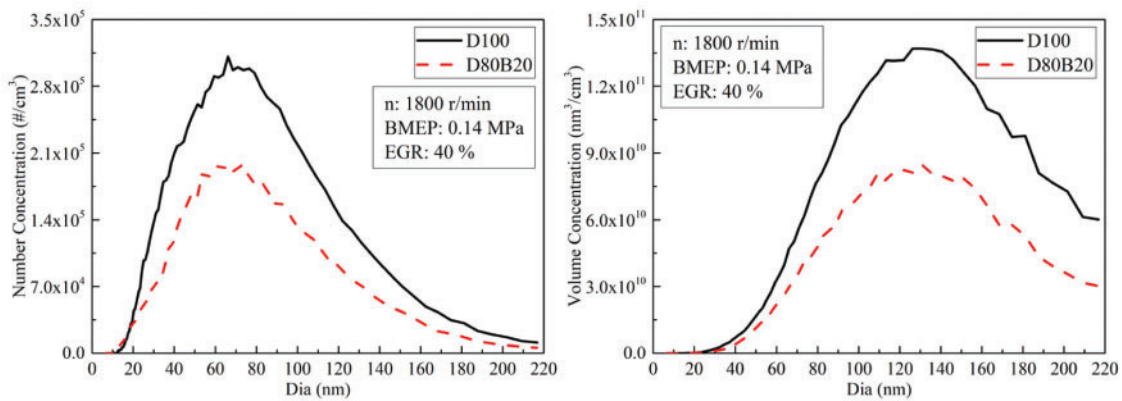
Figure 9: (Continued)



(b) BMEP=0.14 MPa, EGR=20%

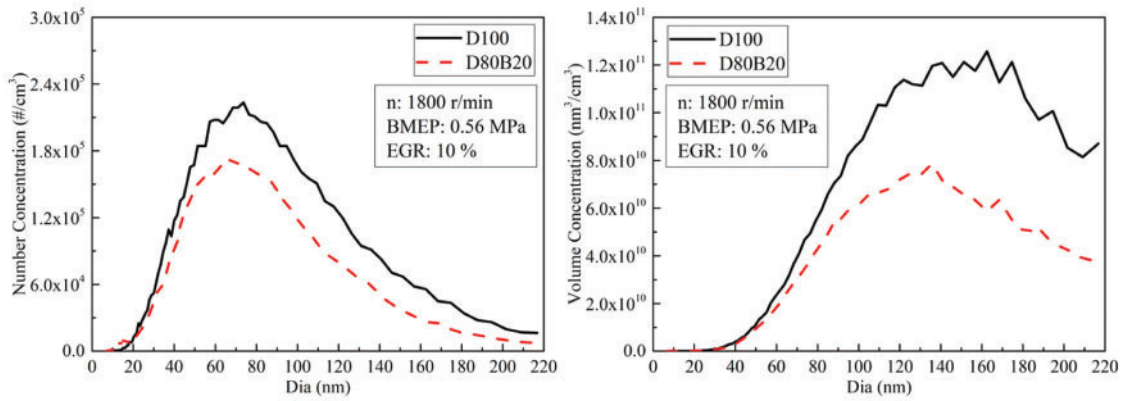


(c) BMEP=0.14 MPa, EGR=30%

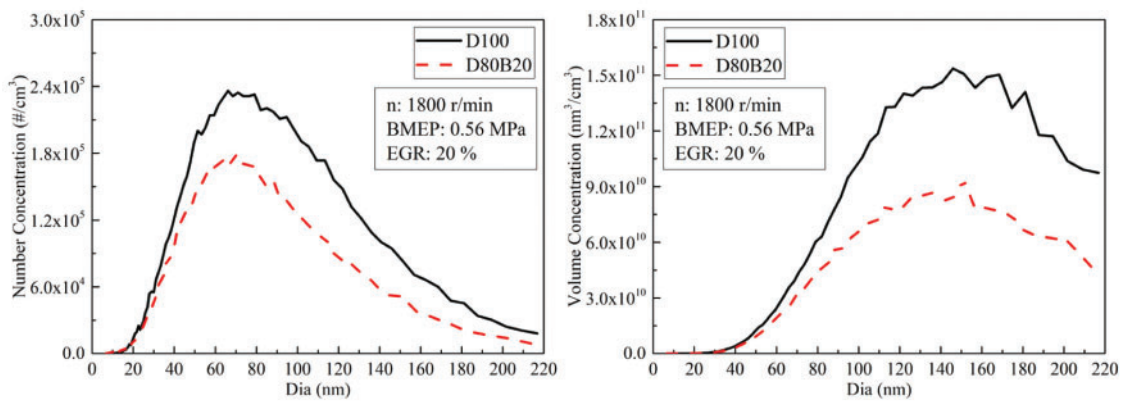


(d) BMEP=0.14 MPa, EGR=40%

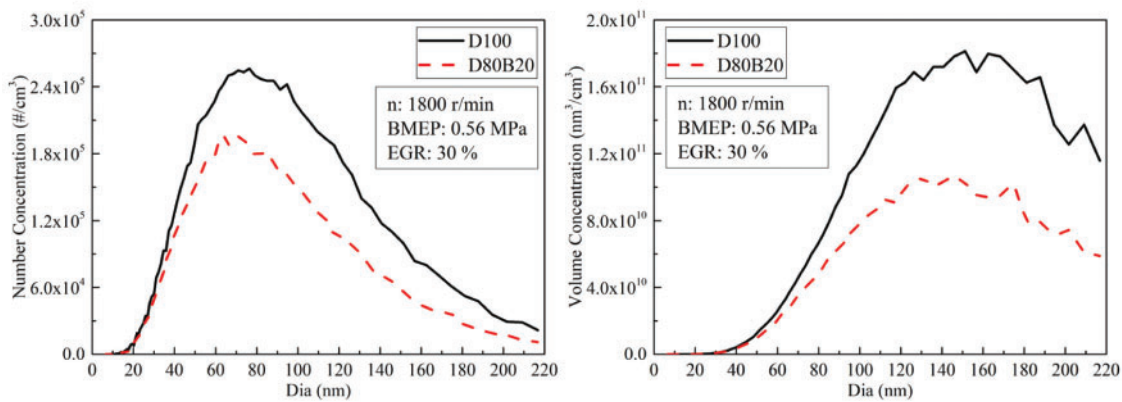
Figure 9: (Continued)



(e)BMEP=0.56 MPa, EGR=10%

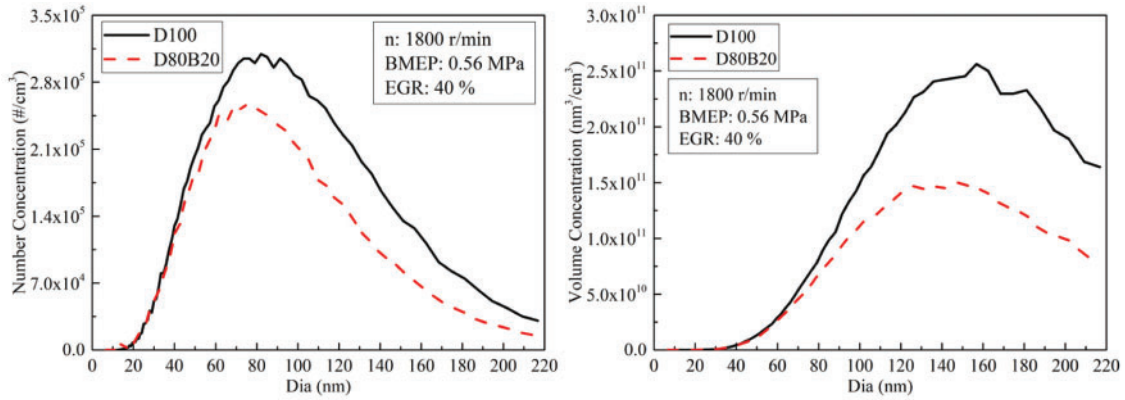


(f)BMEP=0.56 MPa, EGR=20%

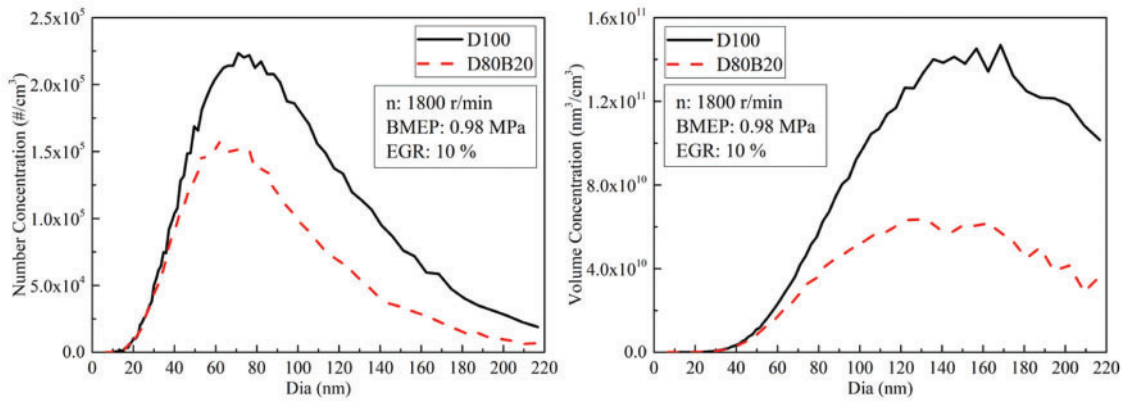


(g)BMEP=0.56 MPa, EGR=30%

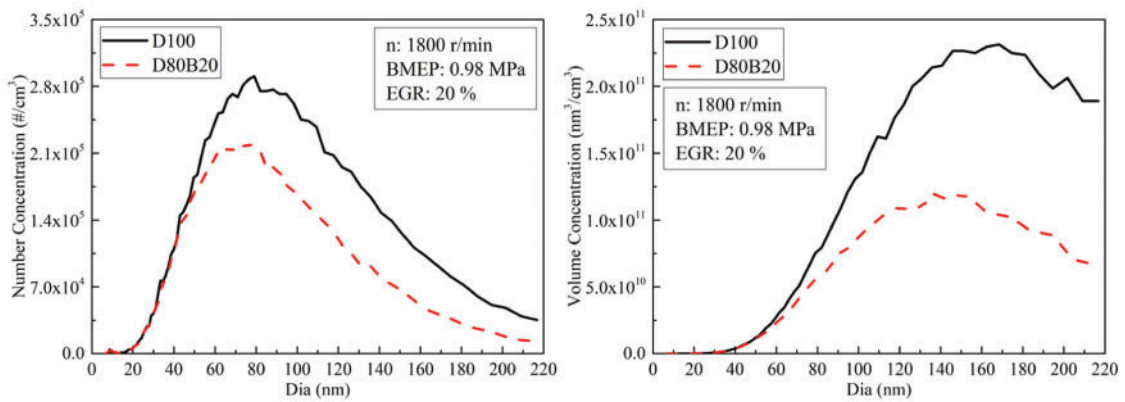
Figure 9: (Continued)



(h) BMEP=0.56 MPa, EGR=40%



(i) BMEP=0.98 MPa, EGR=10%



(j) BMEP=0.98 MPa, EGR=20%

Figure 9: (Continued)

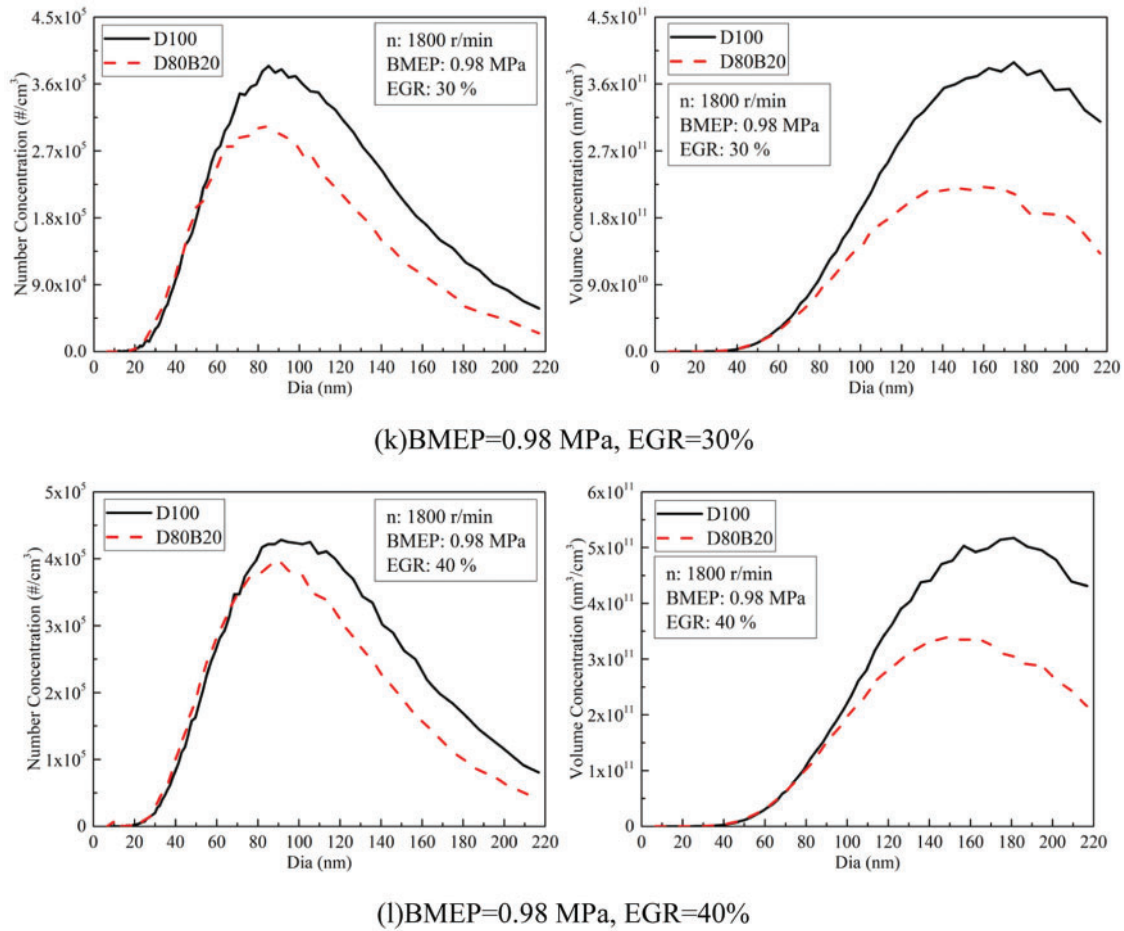


Figure 9: Effects of EGR ratios on NCs and VCs diameter distributions of UFPs

Table 8: The NGMDs and VGMDs of test fuels

BMEP (MPa)	EGR (%)	NGMD (nm)		VGMD (nm)	
		D100	D80B20	D100	D80B20
0.14	0	58	57.3	116	113.9
	10	59.3	57.3	116.2	113.6
	20	60.8	57.3	116.2	113.7
	30	62.7	58.5	115.8	113.6
	40	64	59.7	115.7	112.9
0.42	0	64.6	56	119.5	111.8
0.56	0	71.5	60	123.9	112.1
	10	75.1	64.3	124.1	115.8
	20	75.4	66.1	124.9	119.7
	30	73.7	68	127.2	121.6

(Continued)

Table 8 (continued)

BMEP (MPa)	EGR (%)	NGMD (nm)		VGMD (nm)	
		D100	D80B20	D100	D80B20
0.7 0.84 0.98	40	79.8	71.5	132.5	122.7
	0	73.3	63	123	117.7
	0	76.2	60.6	125.4	114.1
	0	80	58.8	126.6	114.7
	10	84.1	64.4	130.5	116.2
	20	86.8	70	134.8	122.1
	30	87.7	78	137	129.4
	40	90.3	84.2	139.4	133.5

5 Conclusions

N-butanol can be dissolved in diesel, forming stable and homogeneous blend fuel. Blending n-butanol in diesel can effectively improve the combustion quality and decrease the UFPs emission of diesel engines due to its excellent properties and high oxygen content.

- (1) For each fixed EGR ratio, D80B20 has longer ID, shorter CD and thereby higher in-cylinder temperature than D100. Further, D80B20 has lower UFPs emissions but higher NO_x emissions. At 0.70 MPa BMEP, the ultra-fine particle number concentration and ultra-fine particle volume concentration of D80B20 decreased by 31.1% and 46.4% respectively compared with D100.
- (2) Both D100 and D80B20 yield less NO_x emissions as the increase of EGR rate. At 0.98 MPa BMEP, NO_x emissions of D80B20 with 40% EGR ratio decreased by 40.4% compared to that without EGR. As EGR ratio increases, UFPs emissions increase, similarly, the NGMDs and VGMDs of UFPs also increase.
- (3) At 0.14 MPa BMEP and 0.56 MPa BMEP, D80B20 with 20% EGR ratio can reduce both NO_x and UFPs emissions simultaneously. At 0.98 MPa BMEP, D80B20 with 20% EGR ratio can significantly reduce NO_x emissions while UFPs emissions are also at a low level.

Funding Statement: The paper is supported by Innovation Capability Support Program of Shaanxi (Hao Chen received the Grant and Grant No. is 2021TD-28) and Key Research and Development Program of Shaanxi (Hao Chen received the Grant and Grant No. is 2019ZDLGY15-07).

Conflicts of Interest: The authors declare that they have no conflicts of interest to report regarding the present study.

References

1. Liu, Z., Ge, Y., Tan, J., He, C., Shah, A. N. et al. (2012). Impacts of continuously regenerating trap and particle oxidation catalyst on the NO₂ and particulate matter emissions emitted from diesel engine. *Journal of Environmental Sciences*, 24(4), 624–631. DOI 10.1016/S1001-0742(11)60810-3.
2. Yang, X., Fei, H., Xie, W. (2017). NO_x emission on-line measurement for the diesel engine based on tunable diode laser absorption spectroscopy. *Optik*, 140, 724–729. DOI 10.1016/j.ijleo.2017.05.004.

3. Chen, Z. H., Wu, Y. F., Wang, P. L., Wu, Y. P., Li, Z. Y. et al. (2016). Autophagy is essential for ultrafine particle-induced inflammation and mucus hyperproduction in airway epithelium. *Autophagy*, 12(2), 297–311. DOI 10.1080/15548627.2015.1124224.
4. Downward, G. S., van Nunen, E. J., Kerckhoffs, J., Vineis, P., Brunekreef, B. et al. (2018). Long-term exposure to ultrafine particles and incidence of cardiovascular and cerebrovascular disease in a prospective study of a Dutch cohort. *Environmental Health Perspectives*, 126(12), 127007. DOI 10.1289/EHP3047.
5. Kinnunen, T., Matilainen, P., Scheder, D., Czika, W., Waters, D. et al. (2012). Particle oxidation catalyst (POC[®])-from diesel to gdi-studies on particulate number and mass efficiency. *SAE Technical Paper*, 1, 845. DOI 10.4271/2012-01-0845.
6. Chen, H., Su, X., He, J., Zhang, P., Xu, H. et al. (2021). Investigation on combustion characteristics of cyclopentanol/diesel fuel blends in an optical engine. *Renewable Energy*, 167, 811–829. DOI 10.1016/j.renene.2020.11.155.
7. Prasad, K. S., Rao, S. S., Raju, V. R. K. (2019). Performance and emission characteristics of a DI-CI engine operated with n-butanol/diesel blends. *Energy Sources, Part A: Recovery, Utilization, and Environmental Effects*, 1–12. DOI 10.1080/15567036.2019.1685611.
8. Žaglinskis, J., Lukács, K., Bereczky, Á. (2016). Comparison of properties of a compression ignition engine operating on diesel–biodiesel blend with methanol additive. *Fuel*, 170, 245–253. DOI 10.1016/j.fuel.2015.12.030.
9. Zhu, L., Cheung, C. S., Zhang, W. G., Huang, Z. (2010). Emissions characteristics of a diesel engine operating on biodiesel and biodiesel blended with ethanol and methanol. *Science of the Total Environment*, 408(4), 914–921. DOI 10.1016/j.scitotenv.2009.10.078.
10. Chen, H., Su, X., Li, J., Zhong, X. (2019). Effects of gasoline and polyoxymethylene dimethyl ethers blending in diesel on the combustion and emission of a common rail diesel engine. *Energy*, 171, 981–999. DOI 10.1016/j.energy.2019.01.089.
11. Chen, H., He, J., Chen, Z., Geng, L. (2021). A comparative study of combustion and emission characteristics of dual-fuel engine fueled with diesel/methanol and diesel-polyoxymethylene dimethyl ether blend/methanol. *Process Safety and Environmental Protection*, 147, 714–722. DOI 10.1016/j.psep.2021.01.007.
12. Kumar, B. R., Saravanan, S. (2016). Use of higher alcohol biofuels in diesel engines: A review. *Renewable and Sustainable Energy Reviews*, 60, 84–115. DOI 10.1016/j.rser.2016.01.085.
13. Babu, V., Murthy, M. (2017). Butanol and pentanol: The promising biofuels for CI engines—A review. *Renewable and Sustainable Energy Reviews*, 78, 1068–1088. DOI 10.1016/j.rser.2017.05.038.
14. Li, F., Yi, B., Song, L., Fu, W., Liu, T. et al. (2018). Macroscopic spray characteristics of long-chain alcohol-biodiesel fuels in a constant volume chamber. *Proceedings of the Institution of Mechanical Engineers, Part A: Journal of Power and Energy*, 232(2), 195–207. DOI 10.1177/0957650917721336.
15. Wu, J., Zhu, L. L., Wang, Z. C., Xu, B., Wang, H. M. (2014). Experimental study of the spray characteristics of n-butanol/diesel blends. *Advanced Materials Research*, 960, 1394–1399. DOI 10.4028/www.scientific.net/AMR.960-961.1394.
16. Li, F., Yi, B., Fu, W., Song, L., Liu, T. et al. (2019). Experimental study on spray characteristics of long-chain alcohol-diesel fuels in a constant volume chamber. *Journal of the Energy Institute*, 92(1), 94–107. DOI 10.1016/j.joei.2017.11.002.
17. Yi, B., Fu, W., Song, L., Li, F., Liu, T. et al. (2019). Experimental study of the effect of n-butanol additive on spray characteristics of biodiesel in a high-pressure common-rail injection system. *Proceedings of the Institution of Mechanical Engineers, Part A: Journal of Power and Energy*, 233(2), 211–220. DOI 10.1177/0957650918784694.
18. Wang, Q., Sun, W., Guo, L., Fan, L., Cheng, P. et al. (2019). Effects of EGR and combustion phasing on the combustion and emission characteristic of direct-injection CI engine fueled with n-butanol/diesel blends. *Energy Procedia*, 160, 364–371. DOI 10.1016/j.egypro.2019.02.169.

19. Zhou, X., Qian, W., Pan, M., Huang, R., Xu, L. et al. (2020). Potential of n-butanol/diesel blends for CI engines under post injection strategy and different EGR rates conditions. *Energy Conversion and Management*, 204, 112329. DOI 10.1016/j.enconman.2019.112329.
20. Chen, Z., Liu, J., Han, Z., Du, B., Liu, Y. et al. (2013). Study on performance and emissions of a passenger-car diesel engine fueled with butanol–diesel blends. *Energy*, 55, 638–646. DOI 10.1016/j.energy.2013.03.054.
21. Siwale, L., Kristóf, L., Adam, T., Bereczky, A., Mbarawa, M. et al. (2013). Combustion and emission characteristics of n-butanol/diesel fuel blend in a turbo-charged compression ignition engine. *Fuel*, 107, 409–418. DOI 10.1016/j.fuel.2012.11.083.
22. Nabi, M. N., Zare, A., Hossain, F. M., Bodisco, T. A., Ristovski, Z. D. et al. (2017). A parametric study on engine performance and emissions with neat diesel and diesel-butanol blends in the 13-mode european stationary cycle. *Energy Conversion and Management*, 148, 251–259. DOI 10.1016/j.enconman.2017.06.001.
23. Zhang, Q., Yao, M., Zheng, Z., Liu, H., Xu, J. (2012). Experimental study of n-butanol addition on performance and emissions with diesel low temperature combustion. *Energy*, 47(1), 515–521. DOI 10.1016/j.energy.2012.09.020.
24. Atmanlı, A., Ileri, E., Yüksel, B. (2015). Effects of higher ratios of n-butanol addition to diesel–vegetable oil blends on performance and exhaust emissions of a diesel engine. *Journal of the Energy Institute*, 88(3), 209–220. DOI 10.1016/j.joei.2014.09.008.
25. Nayyar, A., Sharma, D., Soni, S. L., Mathur, A. (2017). Experimental investigation of performance and emissions of a VCR diesel engine fuelled with n-butanol diesel blends under varying engine parameters. *Environmental Science and Pollution Research*, 24(25), 20315–20329. DOI 10.1007/s11356-017-9599-8.
26. He, J., Chen, H., Geng, L., Xie, B., Zhao, X. et al. (2019). Investigation on combustion and emission characteristics of diesel and gasoline blends with exhaust gas recirculation. *Energy Sources, Part A: Recovery, Utilization, and Environmental Effects*, 1–15. DOI 10.1080/15567036.2019.1651796.
27. Krieger, R. B. (1966). The computation of apparent heat release for internal combustion engines. *ASME Paper 66-WA/DGP-4*. <https://ci.nii.ac.jp/naid/10003779617/>.
28. Ghojel, J., Honnery, D. (2005). Heat release model for the combustion of diesel oil emulsions in DI diesel engines. *Applied Thermal Engineering*, 25(14–15), 2072–2085. DOI 10.1016/j.applthermaleng.2005.01.016.
29. Wüning, J. A., Wüning, J. G. (1997). Flameless oxidation to reduce thermal NO_x-formation. *Progress in Energy and Combustion Science*, 23(1), 81–94. DOI 10.1016/S0360-1285(97)00006-3.
30. Hoekman, S. K., Robbins, C. (2012). Review of the effects of biodiesel on NO_x emissions. *Fuel Processing Technology*, 96, 237–249. DOI 10.1016/j.fuproc.2011.12.036.
31. Chen, H., Xie, B., Ma, J., Chen, Y. (2018). NO_x emission of biodiesel compared to diesel: Higher or lower? *Applied Thermal Engineering*, 137, 584–593. DOI 10.1016/j.applthermaleng.2018.04.022.
32. Twigg, B. M. V., Phillips, P. R. (2009). Cleaning the air we breathe-controlling diesel particulate emissions from passenger cars. *Platinum Metals Review*, 53(1), 27–34. DOI 10.1595/147106709X390977.
33. Sarathy, S. M., Vranckx, S., Yasunaga, K., Mehl, M., Oßwald, P. et al. (2012). A comprehensive chemical kinetic combustion model for the four butanol isomers. *Combustion and Flame*, 159(6), 2028–2055. DOI 10.1016/j.combustflame.2011.12.017.